Theor Chem Acc (2009) 123:51–58
DOI 10.1007/s00214-009-0548-6

REGULAR ARTICLE

A Bohmian total potential view to quantum effects. II: decay of temporarily trapped states

María F. González · Antoni Aguilar-Mogas · Javier González · Ramon Crehuet · Josep M. Anglada · Josep Maria Bofill · Xavier Giménez

Received: 13 February 2009 / Accepted: 13 February 2009 / Published online: 6 March 2009

Abstract Formation, persistence and decay of temporarily trapped states, the time-dependent generalization of resonances, are analysed within the framework of Bohmian Mechanics. More specifically, the so-called Bohm's total potential, the sum of classical plus Bohm's quantum potential, is used. It is found that both formation and decay are triggered by the frequency in the oscillations of the total potential. These oscillations have been studied at the specific locations where the classical potential displays maxima, i.e. the 'walls' temporarily capturing the system's density. Our main result is that the total potential oscillation frequency is solely dependent on the steepness of the classical potential ramp and, surprisingly, independent of the classical barrier height and width, well depth and width, collision energy or wavepacket width.

Dedicated to Professor Santiago Olivella on the occasion of his 65th birthday and published as part of the Olivella Festschrift Issue.

J. González · R. Crehuet · J. M. Anglada
Institut de Química Avançada de Catalunya,
Consejo Superior de Investigaciones Científicas,
Jordi Girona, 18, 08034 Barcelona, Spain

J. M. Bofill
Departament de Química Orgànica, Universitat de Barcelona,
Barcelona, Spain

M. F. González · A. Aguilar-Mogas · X. Giménez
Departament de Química Física, Universitat de Barcelona,
Barcelona, Spain

M. F. González · A. Aguilar-Mogas · J. M. Bofill · X. Giménez (✉)
Institut de Química Teòrica i Computacional (IQTCUB),
Universitat de Barcelona, Martí i Franquès,
1, 08028 Barcelona, Spain
e-mail: xgimenez@ub.edu

Keywords Bohmian mechanics · Resonances · Quantum dynamics

1 Introduction

Resonances in the microscopic world, i.e. temporarily trapped, or metastable, atomic or molecular states, are manifest, among other phenomena, in radiation–matter spectra, photochemistry, particle physics, laser cooling of atomic species, gas-surface processes and chemical reactions [1–14]. Wave interference is at the heart of resonances. For instance, the radiation–matter wave interference, leading to Einstein's resonance condition, is readily evidenced, formally, in the time dependent perturbation theory formulation of radiation–matter interaction [1]. However, the particle–particle wave interactions leading to resonances, in both particle physics and chemical reactions, are more intringuing. One finds *signatures* of resonances, as bumps in cross sections, or even spikes and other structures in reaction probabilities [4]. But one does not have available a simple ab initio treatment leading to resonances; rather, they are built-in in the basic mathematical structure of the Schrödinger equation. One of the major difficulties is the need of singling out a proper set of adiabatic, or nearly adiabatic, motions, so that one can construct effective potential energy diagrams that, eventually, lead to resonances via an energy match between a forcing projectile's energy, and quasi-bound target energy levels supported by *local* effective potential minima [7].

The characterization of resonances is mostly done under a time-independent picture, even though the main concept is that of decay or, actually, delay *time*. This is because this decay time may be determined by a resonance width in energy space; the larger the width the shorter the lifetime of

the resonance. Within the time-independent version of the Schrödinger equation, this characterization may be done by means of a complex, but otherwise definite, energy. Its real part establishes the position of the resonance, in the energy continuum, whereas the complex part denotes the resonance lifetime [3].

However, the time-independent resonance scheme appears somewhat incomplete since time-independent technology is actually used for the characterization of an intrinsic time-dependent (TD) process. An obvious way to circumvent this is to use the time-dependent, wavepacket (WP) approach to quantum dynamics. A widespread procedure is to Fourier transform the numerical outcome of wavepacket propagation, down in the asymptotic region, and then extract the fixed-energy quantities so as to recover the standard theoretical framework [3]. But it appears that some of the wavepacket time-dependent features are irreversibly mixed up with this Fourier transform. For instance, it is not easy to analyse the role of wavepacket width, as well as wavepacket spreading, under the time-independent picture.

The above shortcomings prompted notorious attempts on the characterization of resonances under a complete time-dependent, wavepacket framework. Noteworthy in this regard are restricted norm techniques or the method of the resonant time correlation function [14, 15]. The present work has been devised to provide yet further material on the time-dependent characterization of temporarily trapped states. These states might be considered as energy-averaged generalizations of resonances, within a simple time-dependent picture. In this work, Bohm's total potential, the sum of classical plus Bohm's quantum potential, is used. This means a shifting from Schrödinger's to Bohm's view of quantum mechanics [15–20]. The latter is intrinsically time-dependent, and well-known to provide a *classical-like descriptive framework* for the occurrence of quantum phenomena.

This work is thus a continuation of a previous study by some of the authors, aimed at viewing quantum effects, in molecular processes, under the perspective of Bohm's total potential [21]. The motivation for such study arises from the absence of knowledge, in the previous literature, on the behaviour of Bohm's total potential associated to standard molecular processes. The ultimate interest is gaining qualitative insight into classical-like descriptions of purely quantum phenomena.

Previous studies by some of the authors have shown that decay processes, under a time-dependent, wavepacket framework, proceed through step-wise increases of the TD density in the decay region [21]. Moreover, a correlation between this density increase outside the barrier, and an *oscillating time dependence* of the total potential, at the classical barrier outermost edge, is found. The underlying, classical-like description of dynamics, linked to Bohm's total potential, means that decay may be described in terms of a deterministic, oscillating pattern displayed by the time dependence of the total potential. The issue is then about finding out the origin of the total potential oscillations as a function of time. Preliminary work by the authors [21] linked these oscillations to the wavepacket's density time-dependence (an obvious conclusion since the density is the time-dependent object in the total potential definition).

However, it is not clear what is the origin of both density and total potential time oscillations. In more specific words, one may state the question as follows: which are the wavepacket, and/or the classical potential features, determining the frequency and amplitude of the density, and total potential oscillations?

In this paper, we have undertaken a comprehensive numerical study aimed at finding out an explanation for both the frequency and amplitude in the total potential oscillations. The main result is that the total potential oscillation frequency is only dependent on the steepness of the external potential ramp, as well as independent of the remainder potential energy features, or the wavepacket characteristics.

The remainder of this paper is organized as follows. Sect. 3 presents the method for solving the TD Schrödinger equation and the total potential, along with a description of the numerical implementation, as well as a description of the properties of the wavepacket being checked to find out the origin of the oscillations in the total potential. Results are shown in Sect. 3. Finally Sect. 4 provides the main conclusions and a summary.

2 Theory and numerical implementation

The Madelung, de Broglie, Bohm (MdBB) hydrodynamic view of quantum mechanics (QM) is readily obtained by expressing the amplitude density as $\psi = R \cdot \exp(iS/\hbar)$, $R(x,t)$ and $S(x,t)$ being *real functions* of the coordinates and time, and substituting afterwards for the standard time-dependent Schrödinger equation. A coupled pair of differential equations results for R (whose square results to be the system's density) and the phase S having a structure that closely resembles that for the characteristic equations for the hydrodynamics of a fluid system [16, 17].

$$\frac{\partial S}{\partial t} + \frac{(\nabla S)^2}{2m} - \frac{\hbar^2}{2m}\frac{\nabla^2 R}{R} + V = 0 \tag{1a}$$

$$\frac{\partial R^2}{\partial t} + \nabla \cdot \left(\frac{R^2 \nabla S}{m}\right) = 0 \tag{1b}$$

Furthermore, the so-called Bohm's guidance relation, $\nabla S = p$, being p the linear momentum, makes explicit the strict formal equivalence between Eq. (1a) and the classical Hamilton–Jacobi equation. However, the resulting

dynamics is only classical-like, and not purely classical, owing to the fact that the quantity.

$$Q = -\frac{\hbar^2}{2m}\frac{\nabla^2 R}{R} \tag{2}$$

plays the role of a state-dependent (*via* R), non-local *quantum* potential Q. When added to the classical potential V, it defines a new quantity acting formally as a potential in (1a), the *total potential*:

$$W = V - \frac{\hbar^2}{2m}\frac{\nabla^2 R}{R} \tag{3}$$

Within this view, one thus switches the focus from kinetic, since the quantum potential has its origin in the quantum kinetic operator, to potential energy. The prospective advantage is that motion is then regarded as classical-like, under the influence, however, of a non-classical, yet cumbersome potential, constructed from the guiding ψ-field.

Calculations have been performed from a TD wavepacket propagation, which is obtained by solving the TD Schrödinger equation. Since the total potential is obtained from the classical potential plus the quantum term, this means that we just need the square root of the wavefunction density. Our procedure, having been described elsewhere, is based on a Discrete-Variable Representation, DVR, [22, 23] which leads to an especially simple time propagation algorithm. In matrix form, it is written as

$$\mathbf{y}(t) = \mathbf{L}^{\mathrm{T}}\mathbf{t}\mathbf{L}\mathbf{j}_0 \tag{4}$$

where $\mathbf{y}(t)$ is the vector, of dimension N, containing the total wavefunction at each grid position, at time t, $\mathbf{t}$ is a diagonal matrix with diagonal elements $e^{-iE_j t/\hbar}$, $j = 1,\ldots,N$, $\mathbf{L}$ is the eigenvectors matrix associated with the DVR-stationary basis change, whereas $\mathbf{j}_0$ is the vector corresponding to the initial wavepacket, with components corresponding to its value at each grid position.

3 The computation of Bohm's total potential

The computation of the quantum potential requires evaluating the density R, *as well as its second spatial derivatives*, at any time increment. However, the TD Schrödinger equation just provides the density. Nevertheless, an advantage of the present formulation for the wavefunction time propagation is that, after suitable transformations, it leads to a simple algorithm for the computation of the quantum potential (and thus the total potential) *at any time increment*, *just by doing simple matrix algebra*. To show this, it is worth starting with the operator expression for the present propagation algorithm for the wave function:

$$\psi(x,t) = \hat{A}(t)\varphi_0(x) \tag{5}$$

where, obviously, the matrix form of $\hat{A}(t)$, in terms of expression (4), is given by

$$\mathbf{A}(t) = \mathbf{L}^{\mathrm{T}}\mathbf{t}\mathbf{L} \tag{6}$$

denoting $B = \hat{A}^*\hat{A}$, the squared modulus of the time propagation operator, and performing the quotient in the quantum potential expression, one gets, after some algebra, in atomic units

$$\begin{aligned} Q(x,t) = -\frac{1}{2m}\frac{\nabla^2 R(x,t)}{R(x,t)} &= \frac{1}{8m}R^{-4}\left\{\frac{\partial\varphi_0^*}{\partial x}B\varphi_0 + \varphi_0^* B\frac{\partial\varphi_0}{\partial x}\right\}^2 \\ &- \frac{1}{4m}R^{-2}\left\{\frac{\partial^2\varphi_0^*}{\partial x^2}B\varphi_0 + 2\frac{\partial\varphi_0^*}{\partial x}B\frac{\partial\varphi_0}{\partial x} + \varphi_0^* B\frac{\partial^2\varphi_0}{\partial x^2}\right\} \end{aligned} \tag{7}$$

thus yielding the final working expression for the computation of the quantum potential, in terms of quantities obtained during the time propagation stage. This procedure has the advantage of linking the accuracy in the calculation of the wavefunction spatial derivatives to the intrinsic accuracy of the DVR method. This accuracy should be superior to the estimation of the derivatives by any finite difference method.

4 Results

4.1 Correlation between density and total potential

Previous studies by the authors [24] have shown a correlation between the density increase after the barrier, i.e. the start of the 'leaking' region, and the oscillating time dependence of the total potential at the classical barrier outermost edge. In order to fully characterize this result, we have made additional calculations to study the total potential oscillations and the probability distribution decay outside the well region. To this end, the system so far considered consists of a particle time evolving in the classical potential shown in Fig. 1. This potential is built by adding an Eckart barrier, centred at a given distance, to a repulsive wall potential, so that it simulates a bonding potential that, according to the system's total energy, has the ability to decay through tunnelling. More specifically, this potential is given by the expression.

$$\begin{aligned} V(x) = V_0\mathrm{Exp}\left[-\frac{2(x-a)}{b}\right] - 2\mathrm{Exp}\left[-\frac{(x-a)}{b}\right] \\ + V_1\mathrm{Sech}\left[\frac{x-c}{d}\right]^2 \end{aligned} \tag{8}$$

with $V_0 = 0.125$, $V_1 = 0.4$, $a = 1.0$, $b = 0.4$, $c = 2.5$, $d = 0.05$. The collision corresponds to an initial coherent wavepacket

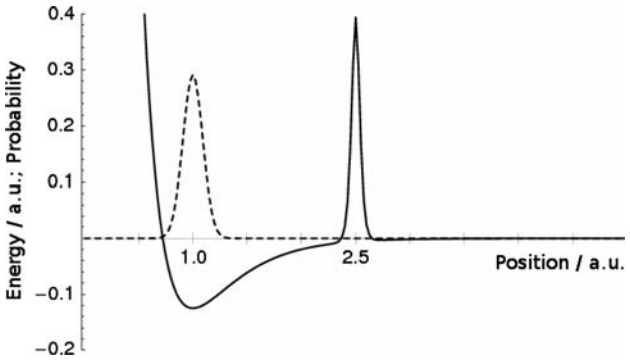

Fig. 1 Potential energy profile used in the present work. Bohm's total potential time oscillations have been studied at the position depicted by P = 2.5 a.u. Atomic units are used throughout

$$\varphi_0(x) = \left(\frac{2\gamma}{\pi}\right)^{1/4} \exp\left\{-\gamma(x-x_0)^2 + ip_0(x-x_0)\right\} \qquad (9)$$

having, $p_0 = 10$, $m = 367.22$ (one-fifth of the proton mass, a quantity taken to ensure purely quantum conditions) and $\gamma = 30$, with initial position $x_0 = 1.0$. Since the barrier height is 0.4 a.u. and the wavepacket central kinetic energy is $p_0^2/2m = 0.1362$ a.u., one may easily assume that any transmission event takes place via tunnelling.

Figure 2 shows four time snapshots of wavepacket time dependence, corresponding to several stages of its oscillation between classical turning points inside the well region. Notice (a) the strongly oscillating pattern for the whole time interval; (b) the presence, at $t = 99$, of an additional effective barrier centred in the well region; (c) the formation of a barrier much higher than the classical, at $t = 109$, and (d) the absence of it at $t = 228$. In addition, it is interesting to note the small tail of the wavepacket, leaking from the well region, even before the first oscillation actually ends. This is a distinctive wavepacket signature of decay, being presented in more detail in Fig. 3. It displays the time dependence of the total potential, at the location where the classical potential displays its barrier maximum, along with the density time dependence, at a point immediately after the barrier. The classical potential barrier height, a constant as a function of time, is also shown for reference. The first important feature shown in this figure is the oscillating character of the total potential time dependence. The classical-like picture of dynamics, linked to the total potential, yields a fairly simple mechanism for resonances: whenever the total potential displays their maxima, the system gets trapped inside the well region, whereas the time ranges where the total potential attain minimum values, the system is allowed to leak from the well region (thus defining proper 'window times' for decay).

It is interesting to notice that the total potential minima occur at ca. 0, 85 and 175 time units. These minima correlate with density maxima taking place at ca. 40, 130 and 225 time units, these delays being explained by the fact that the outgoing density is measured at a point well outside the barrier region and, importantly, the density maxima correspond to optimal constructive interference of the outgoing density. According to the above data, the time distance between successive decay maxima correspond to 90 and 95 time units. This reflects the decreasing mean energy of the leaking wavepacket, at each resonance decay window time, a signature of reflected-wavepacket slowdown resulting from tunneling transmission [25].

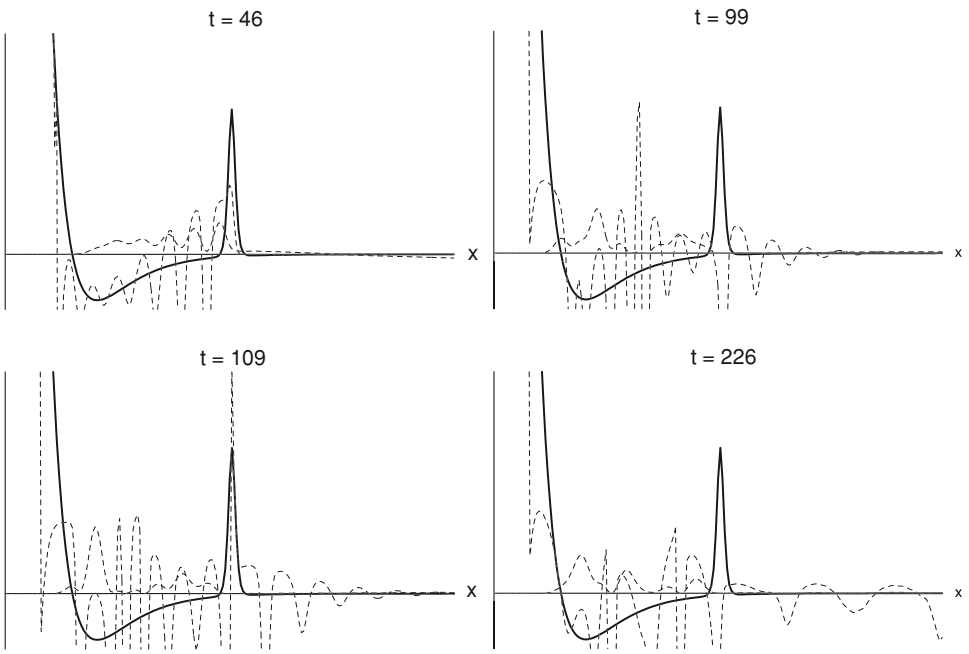

Fig. 2 Wavepacket (*bold dashed line*), total potential (*light line*) snapshots at four selected time instances, for the classical potential (*solid*) depicted in Fig. 1

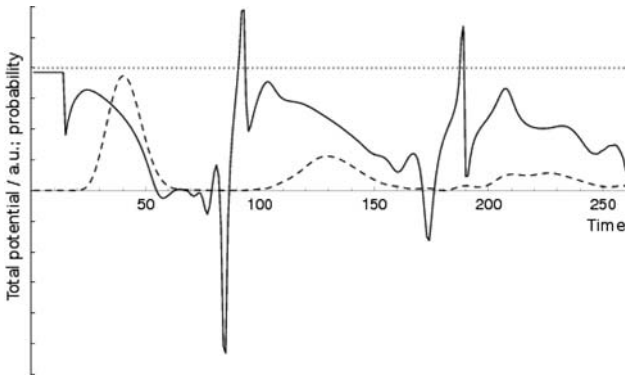

Fig. 3 Total potential (*continuous line*), density (*dashed line*) and classical potential barrier height (*dotted line*), as a function of time. Total and classical potentials correspond to the location of the classical barrier, whereas the density corresponds to a position immediately after the barrier, outside the well region. Some of the potential parameters of Fig. 1 have been slightly changed, in order to get a more clear picture: $V_0 = 0.32$, and $d = 0.114$

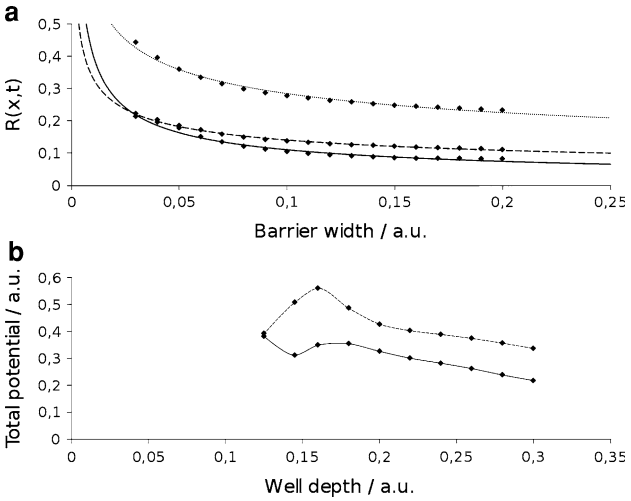

Fig. 4 **a** Density $R(x,t)$ values, for three selected locations ($t = 45$, 135 and 225 time units of Fig. 3), as a function of the barrier width. **b** Total potential values, for two selected locations ($t = 111$ and 225 time units of Fig. 3), as a function of the inner region well depth

4.2 Factors determining the amplitude and frequency of total potential oscillations

Once a general view of the relationship between the total potential and the transmitted density has been obtained for our present system, the study of a family of wavepacket time evolutions, where several of the characterizing parameters of both the wavefunction and the external potential have been systematically changed, is now considered.

Two kinds of quantities have been considered in this section. First, those linked to the wavepacket, namely its central momentum p_0, its width γ, as well as its initial position x_0. Second, quantities corresponding to the classical external potential, i.e. the barrier width and height, the well depth and width, and finally the steepness of the potential slope, i.e. how fast the barrier develops as a function of position.

Interestingly (and counter-intuitively), all the above quantities, except the latest, the potential ramp steepness, leave unaffected the total potential oscillation frequency. This statement, leading to our main result of the present work, is analysed in more detail below. Conversely, the whole set of wavepacket, external classical potential properties are found to act on the oscillation amplitude. The overall trend is complex, even though it can be ascribed to known features of wavepacket dynamics. As an illustration, Fig. 4 shows the density change as the barrier width is varied, along with the change in total potential as the well depth is systematically increased.

Panel (a) of Fig. 4 shows the density $R(x,t)$, as a function of the barrier width, for three selected time instances of the reference density time dependence shown in Fig. 3. These selected $R(x,t)$ points roughly correlate with the density maxima of Fig. 3. The trend for all cases, as the barrier width is increased, is that decaying $R(x,t)$ diminishes, monotonically, as the barrier width is increased. This is an expected result, since in the present work all transmission takes place through tunnelling, and it is well-known that the tunnelling amplitude, for each fixed-energy component of the wavepacket, gets more depleted as the barrier width is larger [26].

A bit more complex is the trend shown in Fig. 4, panel (b). The total potential, for two selected time instances (of the reference time-dependence shown in Fig. 3), first increases (oscillates), and then decreases (in both cases), as the well depth is increased. This behaviour shows how difficult it is to realize, at this point, deeper physical insight. The wavepacket total energy is lowered as the well depth is increased, so that the transmitted density should be monotonically inhibited as the well depth is larger. However, this translates into a non-monotonic behaviour for the total potential.

After varying the parameters characterizing the initial wavepacket and the external potential, the key features governing the total potential are still missing. Some tracks have been found when varying the width of the barrier or its height, two properties which are related to the steepness of the external potential ramp. Hence, we have undertaken the study of how this steepness affects the total potential. This means changing substantially the potential energy parameters, so that, for the sake of simplicity, we have considered other potential profiles than that of Fig. 1. The aim has been to discard the potential profile from any feature not being totally relevant in our study.

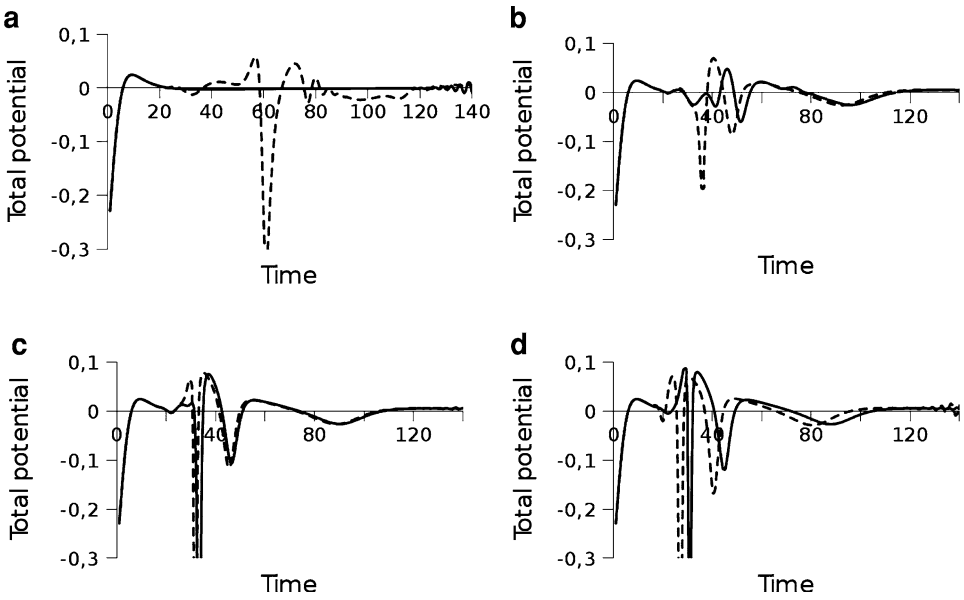

Fig. 5 Total potential for a collision against a linear potential $y = mx$, by a coherent wave packet having $p_0 = 13$, $m_{\text{particle}} = 1836.1/5$ and $\gamma = 20$, with initial position $r_0 = -1$, for different values of the potential slope m. The data have been taken at a point right before the start of the potential ramp. **a** $m = 0$ (*solid*), 1 (*dashed*); **b** $m = 2$ (*solid*), 3 (dashed); **c** $m = 4$ (*solid*), 5 (*dashed*); and **d** $m = 6$ (*solid*), infinite (vertical ramp) (*dashed line*)

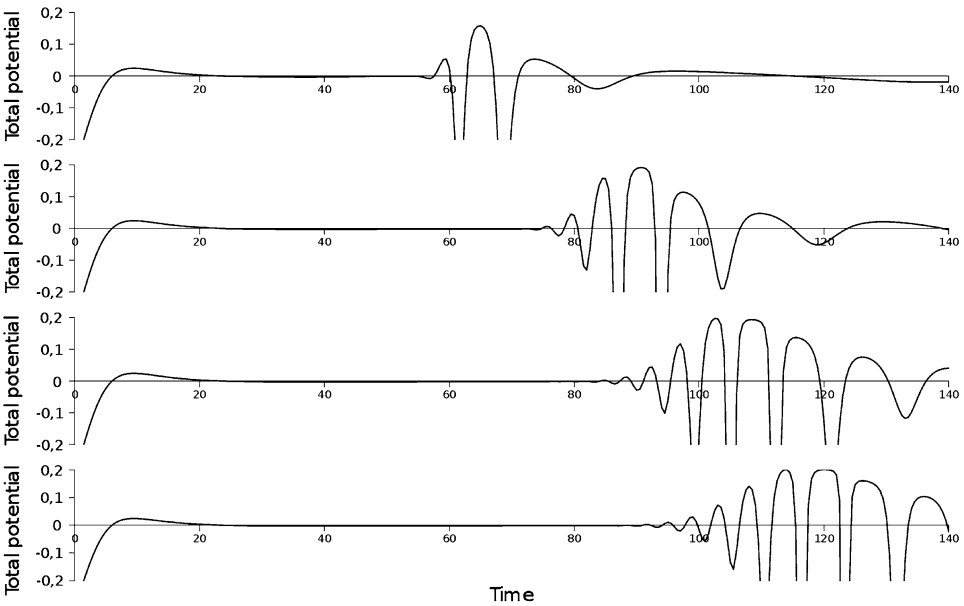

Fig. 6 Total potential time dependence, for an initial coherent wave packet collision against potential ramps defined according to the polynomial equations $V(x) = x^n$, for several values of n. The data have been collected at a point right before the origin of the potential ramps

To this end, Fig. 5, shows the total potential oscillations for an initial coherent wavepacket collision, against a linear potential ramp given by the simple linear term $V(x) = mx$, using different values of the slope m. The data, i.e. the total potential time dependence, have been collected at a point right before the start of the potential ramp, since in the present case the "exit" point taken in the potential profile of Fig. 1 is meaningless. It is found that, as the slope m of the potential ramp is changed, the frequency in the total potential time dependence changes, but the number of oscillations does not change. On the other hand, the oscillation amplitude increases as m is increased.

Finally, Fig. 6 shows the total potential versus time for a wavepacket collision against potential ramps described by simple power functions, $V(x) = x^n$, calculated at a point right before the start of the power-law potential slope. The only change between different ramps is in the power-law degree, n. As a general feature, it is found again that the oscillation frequency changes with n. However, contrary to the linear case, for the time interval so far explored, the number of oscillations is found to change with n.

The specific analysis, concerning the number of oscillations, may be pushed a little bit farther. It starts with the $n = 2$ case. Here the total potential displays four maxima and four minima, as a function of time. Next, the maximum displayed by the figure at *ca.* $t = 65$, is taken as a reference point. This is done since it shows a particular shape, which is reproduced in the remaining cases. Before the reference

maximum, the total potential displays 2 maxima, or crests. For $n = 3$, the number of maxima increases to 4, whereas for $n = 4$ this number increases to 6 and for $n = 5$ it increases to 8. Using higher order polynomials we have verified, numerically, that a simple relation between the number of maxima N_{max} before the reference maximum, is related with the power-law degree n, for $n \geq 2$ by the expression $N_{max} = 2(n - 1)$.

5 Summary and conclusions

The present work is devoted to resonance decay in the context of Bohmian mechanics. In particular, a specific potential energy profile, leading to the formation of a long-living complex, has been considered. The time dependence of a gaussian wavepacket, leading to resonance decay, has been compared to the time dependence of Bohm's total potential. It is found that long-time oscillations in the total potential, at the exit point for resonance decay, actually trigger the system leaking towards the scattering region.

Our main goal has been, consequently, the characterization of these oscillations in the total potential, as a function of the key parameters governing the collision outcome. In particular, the total potential oscillation frequency and amplitude have been studied as a function of wavepacket features, namely the wp central momentum and width, as well as a function of the potential profile characteristics, namely the potential well depth and width, the barrier height and width, as well as the potential ramp steepness.

A main result of the present study is that the total potential oscillation frequency is independent of the wavepacket central momentum p_0, the wavepacket width γ, as well as the classical potential features such as the barrier width and height, and the well depth the well width. Interestingly, it is solely the steepness of the potential ramp that feature which is able to change the oscillation frequency, and consequently, the only feature setting the clock times at which the system decays at sufficiently long collision times. The remaining properties of the system change the oscillation amplitude, i.e. how much the system is decaying at the "clock times" set by the frequency.

Consequently, we are in a position of providing, under the bohmian mechanics framework, a deterministic mechanism for resonance decay (or, more generally, decay of temporarily trapped densities):

a. Decay takes place owing to a time-dependent oscillation of the total potential barrier, which is characterized by a nearly constant frequency. This frequency is dependent solely on the steepness of the classical potential slope leading to the outermost barrier; the higher the frequency the steeper the potential.
b. The remaining system properties determine the amount of decay, i.e. how much of the density gets off the trapping region, at the regular instances set by the total potential oscillation frequency.

We have found, in addition, that the radiated backward oscillations are related to the power-law degree of the potential ramp, which could be used as a deterministic, semiquantitative tool in order to understand how and when resonances decay.

Acknowledgments The authors are among several generations of former students of Professor Santiago Olivella. It has been a true honor to have learned from the inspiring environment and mastership provided by him, along nearly four decades, so that dedicating the present work to him is just the minimum we could do as acknowledgement. Thanks a lot, Santiago!. The authors are grateful for the financial support provided by the Spanish *Ministerio de Ciencia y Tecnología*, DGI project CTQ2005-01117/BQU, and in part by the *Generalitat de Catalunya* projects 2005SGR-00111 and 2005SGR-00175, which is fully acknowledged.

References

1. Feynman RP, Leighton RB, Sands M (1963) The Feynman Lecture on Physics. Addison, Reading
2. Nicolis G (1989) Prigogine I exploring complexity: an introduction. Freeman, New York
3. Zhang JZH (1999) Theory and applications of quantum molecular dynamics. World Scientific, Singapore
4. Truhlar DG (ed) (1984) Resonances in electron-molecule scattering, van der Waals complexes and reactive chemical dynamics. ACS symposium series vol C 263, American Chemical Society, Washington
5. Miller WH, Zhang JZH (1991) J Phys Chem 95:12. doi:10.1021/j100154a007
6. Truhlar DG, Kuppermann A (1970) J Chem Phys 52:3841. doi:10.1063/1.1673570
7. Wu SF, Levine RD (1971) Mol Phys 22:881. doi:10.1080/00268977100103201
8. Skodje RT, Skouteris D, Manolopoulos DE, Lee S-H, Dong F, Liu K (2000) Phys Rev Lett 85:1206. doi:10.1103/PhysRevLett.85.1206
9. Miller WH (1995) Faraday Discuss Chem Soc 102:53. doi:10.1039/fd9950200053
10. Kendrick B, Pack RT (1995) Chem Phys Lett 235:291. doi:10.1016/0009-2614(95)00116-L
11. Chao SD, Skodje RT (2002) Theor Chem Acc 108:273. doi:10.1007/s00214-002-0366-6
12. Miller WH (1974) Adv Chem Phys 25:69. doi:10.1002/9780470143773.ch2
13. Child MS (1996) Molecular collision theory. Dover, New York
14. Sanz AS, Miret-Artés S (2007) Phys Rep 451:37. doi:10.1016/j.physrep.2007.08.001
15. Sanz AS, Miret-Artés S (2005) J Chem Phys 122:014702. doi:10.1063/1.1828032
16. Bohm D, Hiley B (1993) The undivided universe. Routledge and Kegan Paul, London
17. Holland PR (1993) The quantum theory of motion. Cambridge University Press, Cambridge
18. Ali MM, Majumdar AS, Home D (2002) Phys Lett A 304:61. doi:10.1016/S0375-9601(02)01353-1

19. Oriols X, Martín F, Suñé J (1996) Phys Rev A 54:2594. doi: 10.1103/PhysRevA.54.2594
20. Bittner ER (2000) J Chem Phys 112:9703. doi:10.1063/1.481607
21. González J, Bofill JM, Giménez X (2004) J Chem Phys 120:10961. doi:10.1063/1.1747869
22. Colbert DT, Miller WH (1992) J Chem Phys 96:1982. doi: 10.1063/1.462100
23. Neuhauser D, Baer M (1989) J Chem Phys 90:4351. doi: 10.1063/1.456646
24. González J, González MF, Bofill JM, Giménez X (2005) J Mol Struct Theochem 727:205. doi:10.1016/j.theochem.2005.02.052
25. González MF, Bofill JM, Giménez X, Borondo F (2008) Phys Rev A 78:032102. doi:10.1103/PhysRevA.78.032102
26. Landauer R, Martin T (1994) Rev Mod Phys 66:217. doi: 10.1103/RevModPhys.66.217